Entropically Driven Formation of Hierarchically Ordered Nanocomposites

Jae-Youn Lee,[1] Russell B. Thompson,[1] David Jasnow,[2] and Anna C. Balazs[1,*]

[1]*Department of Chemical and Petroleum Engineering, University of Pittsburgh, Pittsburgh, Pennsylvania 15261*
[2]*Department of Physics and Astronomy, University of Pittsburgh, Pittsburgh, Pennsylvania 15261*

(Received 12 April 2002; published 23 September 2002)

Using theoretical models, we undertake the first investigation into the rich behavior that emerges when binary particle mixtures are blended with microphase-separating copolymers. We isolate an example of coupled self-assembly in such materials, where the system undergoes a nanoscale ordering of the particles along with a phase transformation in the copolymer matrix. Furthermore, the self-assembly is driven by entropic effects involving all the different components. The results reveal that entropy can be exploited to create highly ordered nanocomposites with potentially unique electronic and photonic properties.

DOI: 10.1103/PhysRevLett.89.155503 PACS numbers: 81.07.Pr, 61.46.+w, 83.80.Uv

The self-assembly of hard and soft components into nanostructured composites can facilitate the development of novel biomimetic [1], photonic [2], and electronic [3,4] materials. By themselves, binary mixtures of hard particles that differ in size or shape can self-assemble into a startling array of ordered structures [5,6]. Soft block copolymers can "microphase separate" into spatially periodic lamellar, cylindrical, spherical, or more complicated mesophases [7]. Using theoretical methods, in this Letter we conduct the first investigations into the cooperative behavior and novel structures that can potentially emerge when these two disparate ordering phenomena are coupled. Focusing on a small volume fraction of bidisperse spheres in AB diblocks, we isolate a system that simultaneously exhibits a structural change in the system of particles and a transformation in the microstructure of the copolymer matrix, creating in a single process a nanocomposite that potentially exhibits unique optoelectronic properties. Furthermore, these morphological changes are driven entirely by entropic effects involving all of the species. Our results indicate that the blending of particle mixtures and block copolymers can be exploited to create materials with new morphologies and functions.

To characterize the diblocks in our system, we let f denote the fraction of A segments per chain. The enthalpic interaction between an A segment and a B segment is described by the dimensionless Flory-Huggins parameter, χ_{AB}. Both the larger (referred to as p_1) and smaller (p_2) spheres are preferentially wetted by the A blocks. That is, the Flory-Huggins interaction parameter between the particles and A is taken as $\chi_{p1A} = \chi_{p2A} = 0$, and the interaction parameter between the different particles and the B species is set equal to χ_{AB} ($\chi_{AB} = \chi_{p1B} = \chi_{p2B} \equiv \chi$). The radii of the p_1 and p_2 particles are denoted by R_1 and R_2, respectively, and are given in units of R_0, the root-mean-square end-to-end distance of the chain. These nanoparticles are comparable in size to the copolymers, and this correspondence of scales contributes to the unique structural organization within these nanocomposites.

To determine the structure of the mixture, we now modify our previous SCF/DFT approach [8–10], which combines a self-consistent field theory (SCF) for diblocks with a density functional theory (DFT) for solid particles. The new free energy functional is

$$\begin{aligned} NF/\rho_0 k_B TV = {} & (\phi_{p1}/\alpha_{p1})\ln(V\phi_{p1}/Q_{p1}\alpha_{p1}) + (\phi_{p2}/\alpha_{p2})\ln(V\phi_{p2}/Q_{p2}\alpha_{p2}) \\ & + (1-\phi_{p1}-\phi_{p2})\ln[V(1-\phi_{p1}-\phi_{p2})/Q_d] \\ & + (1/V)\int dr\{\chi N[\varphi_A(\mathbf{r})\varphi_B(\mathbf{r}) + \varphi_B(\mathbf{r})\varphi_{p1}(\mathbf{r}) + \varphi_B(\mathbf{r})\varphi_{p2}(\mathbf{r})] - w_A(\mathbf{r})\varphi_A(\mathbf{r}) - w_B(\mathbf{r})\varphi_B(\mathbf{r}) \\ & - w_{p1}(\mathbf{r})\rho_{p1}(\mathbf{r}) - w_{p2}(\mathbf{r})\rho_{p2}(\mathbf{r}) + \rho_{p1}(\mathbf{r})\Psi[\bar{\varphi}_{p1}(\mathbf{r}), x_1, x_2] + \rho_{p2}(\mathbf{r})\Psi[\bar{\varphi}_{p2}(\mathbf{r}), x_1, x_2]\}, \end{aligned} \quad (1)$$

where N is the degree of polymerization, ρ_0^{-1} is a segment volume, V is the volume of the system, and x_1 and x_2 are the mole fractions of the p_1 and p_2 particles, respectively. In (1), α_{pi}, for $i = 1, 2$, is the sphere to diblock volume ratio. Self-consistent fields given by $w_A(\mathbf{r})$, $w_B(\mathbf{r})$, $w_{p1}(\mathbf{r})$, and $w_{p2}(\mathbf{r})$ account for interactions in the system, and act on the A and B blocks of the copolymer and the large and small particles, respectively. Q_d, Q_{p1}, and Q_{p2} are partition functions for single diblocks or particles subject to appropriate fields [8]. The local volume fractions of the various species are given by $\varphi_A(\mathbf{r})$, $\varphi_B(\mathbf{r})$, $\varphi_{p1}(\mathbf{r})$, and $\varphi_{p2}(\mathbf{r})$, while $\rho_{p1}(\mathbf{r})$ and $\rho_{p2}(\mathbf{r})$ are the distributions of the centers of the spheres. ϕ_{pi} are total volume fractions

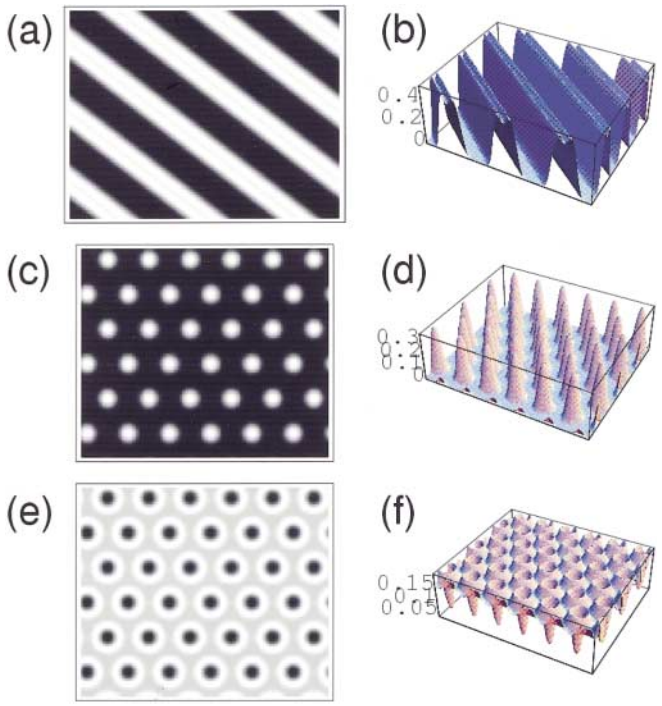

FIG. 1 (color). SCF/DFT density profiles of a spherical particle/diblock copolymer system. In (a)–(f), $\phi_p = 0.2$, $f = 0.3$, and $\chi N = 20.0$. The monodisperse particle case is shown in (a) and (b) as density and surface plots, respectively, where the particle radius is $R = 0.2R_0$. A lamellar morphology is seen. The bidisperse case is shown in (c)–(f), with the large particle ($\phi_{p1} = 0.05$, $R_1 = 0.2R_0$) distribution shown in (c) and (d), while the small particles ($\phi_{p2} = 0.15$, $R_2 = 0.1R_0$) are displayed in (e) and (f). A graded cylindrical morphology results from the introduction of the bidispersity.

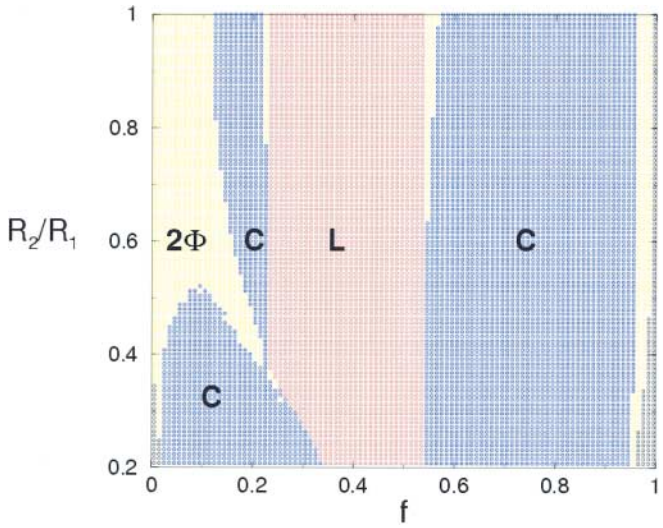

FIG. 2 (color). Phase diagram for mixtures of bidisperse spheres and diblocks calculated using strong segregation theory. R2/R1 is the ratio of the smaller to the larger particle radii and f is the fraction of A units in the diblock. Letters L and C designate lamellar and cylindrical morphologies, respectively. The narrow black regions at the edges of the plot delineate the location of the spherical phases, and the area labeled $2F$ marks the two-phase coexistence region. The total volume fraction of particles is fixed at 20%, of which 3% are the larger and 17% are the smaller spheres. Here, $N = 300$, $\chi_{p1A} = \chi_{p2A} = 0$, and $\chi_{AB} = \chi_{p1B} = \chi_{p2B} = 1$.

of the ith particles. The last two terms in (1) are DFT terms using the expression of Denton and Ashcroft [11]. They account for the steric interactions between the particles. Ψ is the excess free energy per particle, derived from the Mansoori *et al.* equation of state [12]. "Smoothed" densities $\bar{\varphi}_{p1}$ and $\bar{\varphi}_{p2}$ are introduced in the last two terms of (1) using the Tarazona weighted density approximation [13]. Using the SCF method, the mean field free energy (1) is extremized with respect to the fields and densities, under the constraint of incompressibility. The resulting equations are solved numerically and self-consistently to yield the first density profiles of the bidisperse particle/diblock mixture (see Fig. 1).

To demonstrate the generality of our predictions, we herein derive a strong segregation scaling theory (SST) [14,15] for binary mixtures of particles and diblocks (Figs. 2 and 3). In such calculations, the chains are assumed to be highly stretched; the melt is divided into pure-A and pure-B domains, separated by narrowed interfacial regions [14]. The balance between the stretching free energy of the blocks and the energy of the AB interfaces determines the equilibrium morphology of the pure melt. We introduce a volume fraction ϕ_p of A-like particles, of which ϕ_{p1} are larger particles and ϕ_{p2} are the smaller ones. The total volume fraction of diblocks is $\phi_d = (1 - \phi_p)$, where $(f\phi_d)$ is the volume fraction of A monomers and $(1 - f)\phi_d$ is the volume fraction of B units. We assume that the smaller particles can leak into the B domains, with f_2 denoting the fraction in A and $(1 - f_2)$ in B. For simplicity, the smaller particles are assumed to be uniformly distributed within the A and B regions. The larger particles are restricted to the energetically favorable A domains and the distribution of larger particles within A is allowed to vary from uniform to completely segregated [16]. In the latter case, the larger particles are localized near the center of the A domains.

The free energy of the ordered structures is

$$g_{\text{ordered}} = (\phi_d/N)\ln\phi_d + (\phi_{p1}/v_1)\ln(\psi_{1A}) + (f_2\phi_{p2}/v_2)\ln(\psi_{2A}) + [(1 - f_2)\phi_{p2}/v_2]\ln(\psi_{2B}) + \Psi(\psi_{1A}, \psi_{2A}, n_{1A}, n_{2A}) + n_{2B}\Psi_{CS}(\psi_{2B}) + n_{1A}R_1^2/4Nfa_0^2 + n_{2A}R_2^2/4Nfa_0^2 + n_{2B}R_2^2/[4N(1 - f)a_0^2] + \chi(1 - \psi_{2B})\psi_{2B}(0.5/R_2) + 3\phi_d^{2/3}\chi^{1/3}(2N)^{-2/3}\lambda^{2/3}\kappa^{1/3}, \quad (2)$$

where v_i is the volume of a type i sphere, $n_{i\alpha}$ is the number of species i in the α domain, and $a_0 = 1/\sqrt{6}$. R_i is in units of a, the segment length, which is set to 1.

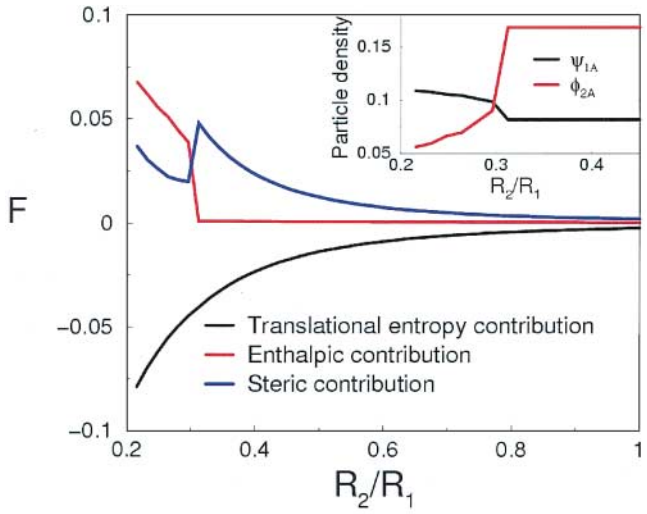

FIG. 3 (color). Decomposition of free energy for bidisperse spheres/diblocks as a function of particle bidispersity calculated using strong segregation theory. Plot is for the same system shown in Fig. 2 at $f = 0.28$. Black curve is the contribution to the free energy from translational entropy, the red curve from the enthalpic interactions, and the blue curve from the steric interaction between particles. The inset shows the fraction of smaller particles in the A phase ($\phi_{2A} = f_2\phi_2$) (red curve) and the local volume fraction of larger particles in the A phase (black curve).

The first four terms describe the translational entropy contributions to the free energy, where ψ_{ia} indicates the local volume fraction of species i in the α domain [15]. The next two terms describe the steric interactions between the particles. The first of the two is the Mansoori *et al.* [12] free energy expression for a binary hard sphere mixture, and the latter is the Carnahan-Starling free energy [17] for the smaller particles in the B phase. For $R_1 = R_2$, the Mansoori term Ψ reduces to the Carnahan-Starling expression for monodisperse spheres. The next three terms are associated with the free energy loss due to the stretching of the chains around the particles. The next term describes the Flory-Huggins interaction between smaller particles and B monomers; the term reduces to the expression for diblocks in solvent when $R_2 = 0.5$. The last term is the diblock contribution to the free energy in the strong segregation limit, where both λ and κ are morphology dependent [14,15]. We consider only the three classical diblock structures: lamellar, cylindrical, and spherical. For each set of parameters for each possible morphology, we minimize Eq. (2) to determine the equilibrium structure. In order to obtain phase diagrams, we compare the free energies of the ordered structures and the disordered phase [18].

Figures 1(a) and 1(b) show the density profiles obtained from the SCF/DFT calculation for $f = 0.30$ and a 20% volume fraction of *monodisperse* particles ($\phi_p = 0.20$) of radius $R = 0.2R_0$. The morphology of the system is clearly lamellar. If we fix f and ϕ_p, but alter the composition of the particle mixture so that there is a 5% volume fraction of larger particles ($\phi_{p1} = 0.05$), with $R_1 = 0.2R_0$, and a 15% volume fraction of smaller particles ($\phi_{p2} = 0.15$), with $R_2 = 0.1R_0$, the system now forms a cylindrical mesophase, as shown in Figs. 1(c)–1(f). These figures also reveal a new structural feature: The large and small A-like particles are not homogeneously distributed. The large particles are concentrated in the center of the domain; in this manner, the A chains do not lose conformational entropy by having to stretch around these large obstacles [8,19]. The smaller particles are concentrated near the edge of the A-B interface and, to a large degree, in the incompatible B phase. In effect, the particles form a "graded" or "gradient" layer, exhibiting a variation in particle size from the center to the edges of the cylinder.

Thus, replacing the monodisperse spheres with an equal volume fraction of bidisperse particles has prompted not only a phase transformation in the polymer microstructure, but also the creation of an inhomogeneous particle distribution within the cylindrical domain. One might say that the system is "hierarchically ordered," having been formed entirely through self-assembly. If the particles are semiconductors, the inhomogeneous layers could display novel optoelectronic properties [20], and the filled cylinders could form an array of nanoelectrodes, which can be utilized to fabricate organized nanodevices [3].

A sufficient disparity in particle size is necessary to produce a transition from the lamellar to the novel cylindrical phase. This can be seen from the phase diagram shown in Fig. 2, which is calculated using the SST approach and plotted as a function of R_2/R_1 and f. Since the SST is primarily applicable at low temperatures, we expect only qualitative agreement between the SST and SCF/DFT calculations. Nevertheless, we can focus on the case where $f \approx 0.3$, as in Fig. 1. At $R_2/R_1 = 1$, within the SST, the system forms a lamellar structure similar to the image in Fig. 1(a). However, it is only for $R_2/R_1 \lesssim 0.3$ that the mixture forms a cylindrical phase; as shown in Fig. 3, the small particles migrate to the B phase, much as in Figs. 1(e) and 1(f).

To determine what drives these morphological changes, we can decompose the different contributions to the total free energy of the system. Since the SST and SCF/DFT give qualitatively similar results, we present results from the SST analysis. Figure 3 shows how the contributions to the free energy from the particles vary as a function of R_2/R_1 at $f = 0.28$. The volume fraction of larger particles is fixed at 3%, while the volume fraction of smaller particles is 17%. The inset shows the volume fraction of smaller particles ($\phi_{2A} = f_2\phi_2$) in the A phase and the local volume fraction of larger particles (ψ_{1A}) in the A phase for various R_2/R_1. ψ_{1A} is a measure of the segregation of the larger particles within the A region; as ψ_{1A} approaches 1, the particles become highly confined in the center of this domain [15].

From the inset, we see that, as R_2/R_1 decreases to approximately 0.3, the smaller particles "delocalize"

and migrate into the energetically unfavorable B regions. This results in an increase in the enthalpic contribution (see Fig. 3); however, this increase in free energy is offset by the gain in the translational entropy of the smaller particles and a decrease in the steric contribution, which is a measure of the crowding of the hard particles. Apparently, entropy wins, and it is more favorable for the particles to be distributed in the manner shown in Figs. 1(c)–1(f) than having the large and small particles uniformly mixed and confined within the energetically favored A phase.

We also note an increase in ψ_1 at the point where the smaller particles delocalize into B (see inset). In mixtures of small and large particles, there is a "depletion attraction" between the larger objects that is due to the extra volume that is available to the smaller particles when the larger particles approach one another, thus increasing the entropy of the system [21,22]. Here, we find similar attractions between the larger spheres; in particular, the "enhanced localization" of the larger particles to the central regions of the A blocks coincides with an increase in the translational entropy of the smaller spheres.

There is a significant consequence of the smaller particles migrating to the B phase. In mixtures involving small monodisperse spheres, the migration of these A-like particles into B apparently decreases the effective value of f and thus can drive the system into the cylindrical phase [23]. It is likely that this mechanism is responsible for the transition from lamellar to cylindrical at $f = 0.28$ and $R_2/R_1 \approx 0.3$ in Fig. 2.

In summary, a number of entropic effects play a role in the observed transition from the lamellar to the cylindrical phase containing the inhomogeneous distribution of particles. Entropic interactions between the A chains and larger particles, and hard sphere interactions between the different particles, drive the larger particles to localize near the center of the A domains. In addition, the smaller particles gain translational entropy by delocalizing and migrating into the unfavorable B phase, suggesting a "microphase separation" in the particle system. Here, we isolated a special case where the fraction of smaller particles in the mixture is relatively high and f is sufficiently close to the order-order transition, that the delocalization of these spheres and the lamellar-cylindrical transition in the matrix structure happen simultaneously.

While our discussion focussed on the structures in Fig. 1, we also find novel structures by altering the relative number of smaller and larger particles at fixed ϕ_p and f. For example, for $\phi_{p1} = 0.15$ and $\phi_{p2} = 0.05$ at $f = 0.30$, we obtain a graded layer of nanoparticles within a lamellar matrix. Thus, the findings point to a new methodology for tailoring the particle distributions within the copolymer matrix and thereby controlling the properties and performance of the nanocomposite. The results also reveal that, in mixtures of hard and soft components, entropy can be exploited to create ordered materials with potentially useful structures.

The authors gratefully acknowledge financial support from the NSF, DOE, and ARO.

*Corresponding author.
Electronic address: balazs1@engrng.pitt.edu

[1] S. I. Stupp and P. V. Braun, Science **277**, 1242 (1997).
[2] Y. Fink, A. M. Urbas, M. G. Bawendi, J. D. Joannopoulos, and E. L. Thomas, J. Lightwave Technol. **17**, 1963 (1999).
[3] E. Jeoung *et al.*, Langmuir **17**, 6396 (2001).
[4] W. A. Lopes and H. M. Jaeger, Nature (London) **414**, 735 (2001), and references therein.
[5] P. Barlett, R. H. Ottewill, and P. N. Pusey, Phys. Rev. Lett. **68**, 3801 (1992), and references therein.
[6] M. Adams, Z. Dogic, S. L. Keller, and S. Fraden, Nature (London) **393**, 349 (1998).
[7] F. Bates and G. Fredrickson, Phys. Today **52**, 32 (1999).
[8] R. Thompson, V. Ginzburg, M. Matsen, and A. C. Balazs, Science **292**, 2469 (2001).
[9] R. Thompson, V. Ginzburg, M. Matsen and A. C. Balazs, Macromolecules **35**, 1060 (2002).
[10] R. Thompson, J. Y. Lee, D. Jasnow, and A. C. Balazs, Phys. Rev. E (to be published).
[11] A. R. Denton and N. W. Ashcroft, Phys. Rev. A **42**, 7312 (1990).
[12] G. A. Mansoori, N. F. Carnahan, K. E. Starling, and T. W. Leland, J. Chem. Phys. **54**, 1523 (1971).
[13] P. Tarazona, Mol. Phys. **52**, 81 (1984).
[14] A. N. Semenov, Sov. Phys. JETP **61**, 733 (1985).
[15] J. Huh, V. Ginzburg, and A. C. Balazs, Macromolecules **33**, 8085 (2000).
[16] Our assumptions about the distributions of the smaller and larger particles are well supported by the SCF/DFT calculations (see Fig. 1).
[17] N. F. Carnahan and K. E. Starling, J. Chem. Phys. **51**, 635 (1969).
[18] The free energy of the disordered phase is:

$$\begin{aligned} g_{\text{disordered}} &= (\phi_d/N)\ln(\phi_d) + (\phi_{p1}/v_1)\ln(\phi_{p1}) \\ &+ (\phi_{p2}/v_2)\ln(\phi_{p2}) \\ &+ \Psi(\phi_{p1}, \phi_{p2}, \phi_{p1}/v_1, \phi_{p2}/v_2) \\ &+ (\phi_{p1}/v_1)R_1^2/4Na_0^2 + (\phi_{p2}/v_2)R_2^2/4Na_0^2 \\ &+ \chi(1-f)(1-\phi_p)\phi_{p2}(0.5/R_2) \\ &+ \chi f(1-f)(1-\phi_p)^2. \end{aligned}$$

[19] Our observation that large spheres localize in the center of the A domains agrees with experimental findings on the behavior of monodisperse nanoparticles in lamellar diblock films [see V. Lauter-Pasyuk *et al.*, Physica (Amsterdam) **241B**, 1092 (1997)].
[20] N. Kotov, MRS Bull. **26**, 992 (2001).
[21] A. D. Dinsmore, A. G. Yodh, and D. J. Pine, Phys. Rev. E **52**, 4045 (1995).
[22] A. D. Dinsmore, A. G. Yodh, and D. J. Pine, Nature (London) **383**, 239 (1996), and references therein.
[23] J. Y. Lee, R. Thompson, D. Jasnow, and A. C. Balazs, Macromolecules **35**, 4855 (2002).